Natural Hazards
https://doi.org/10.1007/s11069-019-03810-1

ORIGINAL PAPER

Investigating relationship between drought severity in Botswana and ENSO

Jimmy Byakatonda[1] · B. P. Parida[2] · Ditiro B. Moalafhi[3] · Piet K. Kenabatho[3] · David Lesolle[3]

Received: 19 August 2016 / Accepted: 2 October 2019

Abstract
Influences of El Niño southern oscillation (ENSO) on weather systems have increased the frequency and amplitude of extreme events over the last century. This even continues to exacerbate the already warming earth, with 2014–2016 which coincided with the strongest El Niño years observed as the warmest period in recent past. This study presents an approach of characterizing droughts at various timescales and establishes teleconnections between ENSO and drought severity in Botswana. The study uses Standardized Precipitation Evaporation Index (SPEI) at timescales of 1, 3, 6, 12 and 24 month to characterize droughts and Pearson's correlations to study the teleconnections between SPEIs and ENSO. Results from the study reveal that extreme droughts are a rare occurrence in Botswana though it is more prone to moderate droughts at 12 month SPEI with a probability of 19% in the north. The highest severe drought probability was 7% recorded in the east. Linear trends indicate increasing dryness of around 0.8% per decade. These results have demonstrated that warm sea surface temperatures combined with negative Southern Oscillation Index correspond to persistent negative SPEI values and thus are likely to result in dry conditions. Significant correlations were observed in the mid austral summer in December and January. Due to this relationship, the drought early warning systems could use ENSO as one of the instruments for predicting drought over the study area and hence in its management.

Keywords Drought vulnerability · Early warning · El Niño · Pearson's correlation · Standardized Precipitation Evaporation Index

✉ Jimmy Byakatonda
byakatondaj@hotmail.com

[1] Department of Biosystems Engineering, Gulu University, P.O Box 166, Gulu, Uganda

[2] Department of Civil Engineering, University of Botswana, P/Bag 0061, Gaborone, Botswana

[3] Department of Environmental Science, University of Botswana, P/Bag 00704, Gaborone, Botswana

Published online: 14 October 2019

1 Introduction

In the recent decades (1980–2014), the world has witnessed a twofold increase in annual rate of weather-related disasters seeking urgent humanitarian aids to both rapid-onset disasters such as floods and slow-onset crises due to droughts, besides others (Conforti et al. 2018). Beyond this, in particular between 2014 and 2016, the world has even observed the warmest period on record with the year 2016 showing highest rise (approximately a rise by 1.1 °C). Such an event has been found to have been facilitated by the strongest El Nino in the past 100 years (Hansen et al. 2016). Further to this, with the ongoing phenomena of climate change, the effects of El Nino which have been attributed to the increased weather-related disasters are likely to continue and bring in more miseries through recurring floods in low lying and droughts in semiarid areas. While combined collateral damage of floods and droughts between the twentieth and twenty-first century is estimated at $850 M on a global scale (Guha-Sapir et al. 2016), droughts have been singled out to be among the world's most devastating natural hazard with far reaching effects on the economy, environment and other livelihoods (Wilhite et al. 2007; Yu et al. 2014; Wang et al. 2015).

Since meteorological droughts (periods of below normal rainfall) are believed to propagate gradually covering more spatial and temporal extent as compared to other natural hazards (Mishra and Singh 2010; Edossa et al. 2014), their onset and cessation are difficult to identify. Even as the meteorological droughts persist, they progress into agricultural drought when soil moisture starts to deplete and hamper agricultural production. With 12–24 month of continuously below normal rainfall, groundwater and streamflow are also affected as droughts progress to hydrological drought (White and Walcott 2009; Sheffield et al. 2012; Yaghoobi 2012; Van Loon 2013).

Since droughts are an integral part of the climate cycle, they may not be avoidable but their impacts can be mitigated through preparedness and monitoring (Narasimhan and Srinivasan 2005; Morid et al. 2007). In an effort to lessen the impact of droughts and make the nations weather ready, the World Meteorological Organization (WMO) has recommended use of drought indices for drought monitoring (WMO 2009). However attainment of successful drought monitoring is dependent on how drought is characterized and quantified in both spatial and temporal extents (Iglesias et al. 2009; Nalbantis and Tsakiris 2009; Lloyd-Hughes 2012; Mbululo and Nyihirani 2012). Drought indices at times are presented as proxies of various environmental systems such as soil moisture storage and stream flow (Heim Jr Heim 2002; Dai 2013). As a result, numerous drought indices have emerged over time to aid classification of drought in form of severity, duration, interval and intensity (Alley 1984; McKee et al. 1993; Trenberth et al. 2007; Vicente-Serrano et al. 2010; Yaghoobi 2012; Beguería et al. 2014; Stagge et al. 2014). Of all these indices, those that are mainly utilized and recommended by the WMO are the Palmar Drought Severity Index (PDSI), Standardized Precipitation Index (SPI) and Standardized Precipitation Evaporation Index (SPEI) (Hayes et al. 2011; Sivakumar et al. 2011).

This study employs SPEI in characterization of drought by duration, severity and intensity. The choice of SPEI was premised on the fact that like the PDSI, it considers potential evapotranspiration (PET) as a predictor of drought severity. At the same time, it considers the multiscalar nature of SPI by incorporating the timescales over which moisture deficiency emanates (Vicente-Serrano et al. 2010; McEvoy et al. 2012; Beguería et al. 2014; Trambauer et al. 2014). The SPEI is a generally accepted drought index that accounts for effects of global warming that cannot be ignored in studies of drought severity. Predictions from climate models in recent times have revealed a possible global temperature rise of up to 2 °C (above the

Paris declaration) in the near future (Feidas et al. 2004; Trenberth et al. 2007; Engelbrecht et al. 2015; Rahman and Lateh 2017). For this reason, global warming could also be a precursor of drought and hence inclusion in this study. Besides in a recent study by Byakatonda et al. (2018b), it was established that SPEI performs better than SPI especially during the winter season in Botswana. In addition to this, many researches have established that ocean–atmosphere dynamics triggered by activities in the equatorial Pacific basin referred to as El Niño southern oscillation (ENSO) are closely linked with global warming and also associated with increased drought severity (Nicholson and Kim 1997; Nicholson et al. 2001; Fauchereau et al. 2003; Nyenzi and Lefale 2006; Trenberth et al. 2007; Vicente-Serrano et al. 2011).

In recent findings, some of which are presented in Vicente-Serrano et al. (2011), they document effect of ENSO on drought severity at a global scale using gridded data. However, there is high uncertainty in global gridded data due to low spatial extent and thus cannot be solely relied upon. There is also inherent spatial variability in rainfall, largely resulting from towering (cumulus) isolated clouds (Yuan and Hartmann 2008). Wang et al. (2015) found differing trends in dryness conditions over China while using ground observed data as compared to other results reported by Dai (2013) and Vicente-Serrano et al. (2011) who used gridded data over the same area. For this reason, this study utilized local observed data to make a comprehensive analysis of the association between drought severity and ENSO. In South Africa Edossa et al. (2014) have conducted drought severity studies using SPEI and found that SPEI was closely linked to SSTs anomalies. However, in that study, oceanic influence at the South African coast cannot be ruled out as compared to the landlocked nature of the study area. To aid understanding of this association, Botswana which is located in semiarid region of Southern Africa is selected. Effects of global warming in Botswana cannot be ignored due to its location. For example, it is generally agreed that under all the IPCC scenarios of climate change, most global climate models (GCMs) project an increase in temperature at various levels. This is likely to lead to perturbation of various aspects of climate, including extreme events, drought inclusive. In the most recent study on temporal variations in meteorological variables by Byakatonda et al. (2018a) in Botswana, it was found out that maximum temperature was highly influenced by activities in the Equatorial Pacific. Currently Botswana does not have systematic monitoring of drought episodes even though effects of droughts are well documented especially in agricultural production. With lack of reliable data on droughts that could inform mitigation strategies, Botswana's government has historically taken a reactive approach to dealing with drought crises (Morchain et al. 2017). A drought year is usually declared following consideration of the drought and household food security assessment and analysis report. In most cases, the drought periods coincided with El Niño Southern Oscillation (ENSO) which can be related to Sea Surface Temperatures (SSTs). It is in this context that this study premises itself on investigating the effects of ENSO specifically on drought severity across Botswana. Considering that Botswana is a water scarce country with most national rivers mainly depending on the local climate, it may be necessary to explore if the local climatic factors expressed as drought severity are influenced by external factors such as ENSO represented by SST anomalies and SOI.

2 Materials and methods

2.1 Study area

The study has been conducted in Botswana which is located in Southern Africa, and the area is classified as semiarid and receives rainfall ranging from 200 to 600 mm annually. Evaporation rates range between 1800 and 2100 mm/year way above the rainfall amounts (FAO 2001; Batisani 2012; Byakatonda et al. 2016). Rains are normally expected in the summer between November and March (Nicholson et al. 2001; Byakatonda et al. 2019). The rains are dominant in the north-east at Kasane then decreases to the west at Ghanzi, and lowest records are registered in the south-west at Tsabong (Fig. 1). The rainfall is highly erratic with coefficient of variation exceeding 25% at all locations as shown in Fig. 1. Variability is highest in the driest areas of Tsabong and Ghanzi. Climate systems over the study area are governed by south-eastern trade winds and the movement of the Inter Tropical Convergence Zone (ITCZ). These climatic systems are heavily linked to conditions of the ENSO events in the equatorial Pacific Ocean (Bepura 1999; Nicholson et al. 2001; Trenberth et al. 2007). It is envisaged that drought events will be more frequent

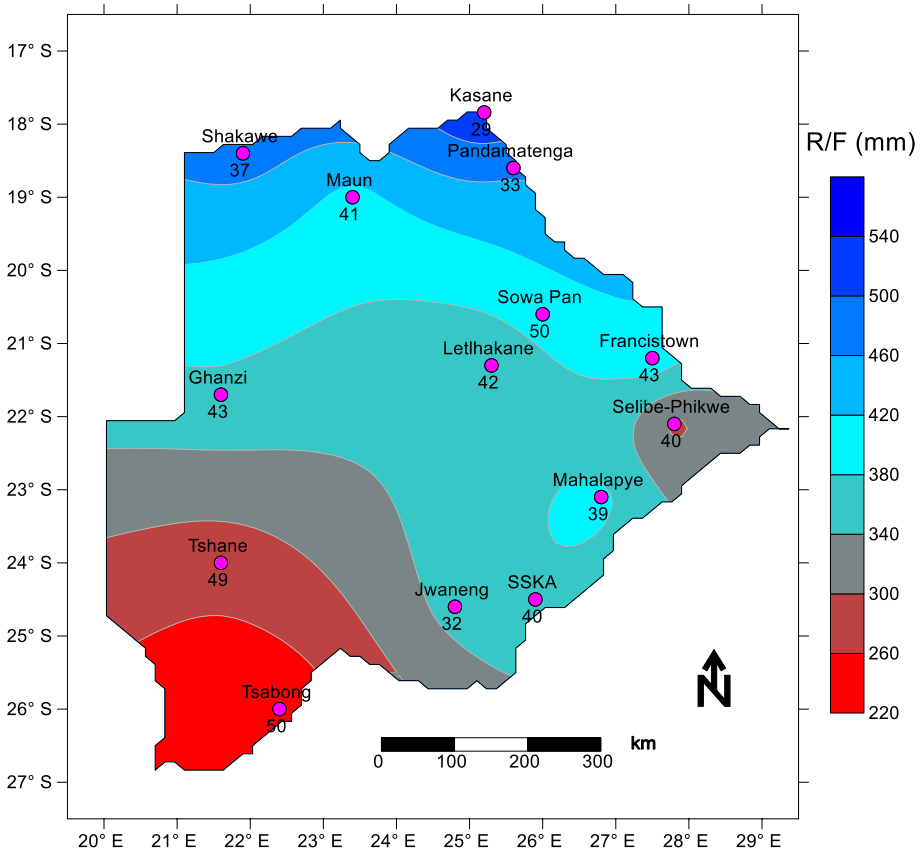

Fig. 1 Meteorological stations and annual rainfall amount (mm) distribution together with their coefficients of variation (CV) over the study area

and higher in magnitude in arid and semiarid areas due to incidences of global warming (Feidas et al. 2004; Franks 2005; Rahman and Lateh 2017). This makes Botswana more drought prone in future hence the need to boost her early warning systems.

2.2 Data

2.2.1 Local climatological data

Records of rainfall, minimum and maximum temperature at monthly timescale were obtained from the Department of Meteorological Services of Botswana (DMS) at fourteen synoptic stations with the longest record being 1960–2016. The stations have a good spread over the study area as presented in Fig. 1. Data on monthly Sea Surface Temperature (SST) anomalies from the El Niño 3.4 region and Southern Oscillation Index (SOI) were obtained from the climate prediction center of the National Oceanic and Atmospheric Administration (NOAA-NCEP 2016) and the National Climate and Data Center of NOAA from NOAA-NCDC (2016), respectively, for a concurrent period of 1960–2016.

The homogeneity of the rainfall and temperature was tested using the standard normal homogeneity test proposed by Alexandersson (1986) and the Pettit test by Pettit (1979). The rainfall time series were found to be fully homogeneous at all the stations used in this study. Some of the stations were found to exhibit inhomogeneity in temperature series for at least one of the tests. These stations were classified as doubtful according to procedure suggested by Wijngaard et al. (2003) and Costa and Soares (2009) and applied in Byakatonda et al. (2018b).

2.3 Large-scale climatic predictors

2.3.1 Sea surface temperature anomalies

El Niño southern oscillation is closely associated with oceanic-atmospheric dynamics that influence variations in ocean currents and SSTs with teleconnections up to the Antarctic (Bromwich et al. 2000). The ENSO phenomena consist of two components of El Niño and La Niña. The latter is linked with cooler SSTs in the east of the equatorial Pacific and for this condition to occur, this event coincides with a strong Walker circulation (Rojas et al. 2014). The El Niño conditions result from warm SSTs in the western Pacific progressing to the east and this phase coinciding with a weak Walker circulation. The main activity of the El Niño (La Niña) occurs when the central equatorial Pacific Ocean is warm (cool) covering the regions between 3 and 4. Strong positive anomalies signify El Niño, whereas strong negative is a precursor to La Niña events.

2.3.2 Southern Oscillation Index (SOI)

Southern Oscillation Index (SOI) also called the Walker circulation defines the east-west atmospheric movement. SOI is applied in the quantification of the ENSO magnitude based on atmospheric pressure. It is computed from the difference between sea level pressure measurement at Tahiti and Darwin (Troup 1965; Rojas et al. 2014). Negative values of SOI are associated with El Niño, while strong positive values are La Nina events. Various studies have associated climatic disasters such as droughts, floods, tsunamis, and hurricanes to ENSO/SOI

that influence variant atmospheric and oceanic behaviours (Usman and Reason 2004; Morid et al. 2007; Trenberth et al. 2007; Vicente-Serrano et al. 2011; Edossa et al. 2014).

2.4 Drought severity characterization using standardized precipitation evapotranspiration index (SPEI)

Drought severity is characterized according to classes presented in Table 1 of standardized indices representing drought severity. The determination of SPEI is summarized in the following steps (Beguería et al. 2014; Edossa et al. 2014; Stagge et al. 2015; Byakatonda et al. 2016).

1. Determination of potential evapotranspiration (PET) and generation of the climatic water balance (W_i) which is the difference between monthly rainfall amounts (R) and potential evapotranspiration (PET).
2. Aggregation of the climatic water balance (W_i) from step (1) over a period of n month, where n is a scale over which drought duration can be measured.
3. The aggregated climatic water balance time series obtained in step (2) are then standardized through a Gaussian transformation.

2.4.1 Computation of potential evapotranspiration

UN-FAO recommends the use Penman–Monteith method for determination of potential evapotranspiration (PET) (Allen et al. 1998; Cai et al. 2007). However, the limitation of this method is large amounts of data required in the computation process, for this study long term records on humidity, sunshine duration and wind velocity required for use in Penman–Monteith equation were not available over the study area. This called for use of an alternative approach of Hargreaves to determine PET. This method has been used in determination of SPEI and found comparable with the Penman Monteith method (Beguería et al. 2014; Edossa et al. 2014; Stagge et al. 2015; Byakatonda et al. 2016). The following equation was used to compute PET:

$$\mathrm{PET} = 9.384 \times 10^{-4} r_{\mathrm{a}} \left(T_{\mathrm{mean}} + 17.8\right) \sqrt{\left(T_{\mathrm{max}} - T_{\mathrm{min}}\right)} \tag{1}$$

where T_{mean} is the mean air temperature (°C), T_{max} is the maximum air temperature (°C), T_{min} is the minimum air temperature (°C) at monthly timescale, and r_{a} is extraterrestrial radiation (MJ m^{-2} d^{-1})

Table 1 Drought severity classifications (Yu et al. 2014)

Drought severity	Drought severity classes
< − 2	Extreme drought
− 1.99 to − 1.50	Severe drought
− 1.49 to 1.00	Moderate drought
− 1.00 to 1.00	Near normal
1.00 to 1.49	Moderately wet
1.50 to 1.99	Severely wet
> 2.00	Extreme wet

2.4.2 Aggregation of climate water balance (W_i) series

The W_i series are accumulated at different timescales of $n=1$, 3, 6, 12 and 24 month. Twelve independent series are generated for each month in order to maintain the homogeneity of the accumulated W_i series (Vicente-Serrano et al. 2010; Yaghoobi 2012; Stagge et al. 2015), the accumulated W_i ($W^n_{j,i}$) in a given month i and year j is dependent upon a selected timescale n. For illustration purposes, the accumulated series for 1 month in a particular year j with $n=12$ is determined from;

$$W^n_{j,i} = \sum_{l=13-n+i}^{12} W_{j-1,l} + \sum_{l=1}^{j} W_{j,l} \quad \text{if } j < n \text{ and} \tag{2}$$

$$W^n_{j,i} = \sum_{l=j-n+1}^{j} W_{j,l} \quad \text{if } j \geq n \tag{3}$$

2.4.3 Standardization of the water balance series

In determining SPEI values, three-parameter distribution was utilized since W_i values can have both negative values in periods of low rainfall and positive values in periods of above normal rainfall (Potop et al. 2010; Vicente-Serrano et al. 2010). L-Moments as linear combinations of ordered $W^n_{j,i}$ series were used for fitting an appropriate probability distribution function on to the original series. L-moments were selected because they are believed to give least bias estimates and performs well even with data sets containing outliers (Hosking and Wallis 2005; Beguería et al. 2014; Byakatonda et al. 2016).

The L-moments allow comparison of various candidate frequency distributions that can fit the $W^n_{j,i}$ series. To identify the candidate distributions, L-moments ratios of L-Skewness (τ_3) and L-Kurtosis (τ_4) were used since they are a summary of probability distributions in terms of the shape, location and scale parameters (Hosking and Wallis 2005). L-Skewness τ_3 and L-Kurtosis τ_4 are presented in Eqs. 4 and 5;

$$\tau_3 = \frac{\lambda_3}{\lambda_2} \tag{4}$$

$$\tau_4 = \frac{\lambda_4}{\lambda_2} \tag{5}$$

λ_1, λ_2, λ_3 and λ_4 are first to fourth-order linear moments obtained from $W^n_{j,i}$ arranged in ascending order. They are computed from Eqs. 6–9 (Hosking and Wallis 2005; Parida and Moalafhi 2008);

$$\lambda_1 = E\left[W^n_{j,i(1:1)}\right] \tag{6}$$

$$\lambda_2 = \frac{1}{2}E\left[W^n_{j,i(2:2)} - W^n_{j,i(1:2)}\right] \tag{7}$$

$$\lambda_3 = \frac{1}{3}E\left[W^n_{j,i(3:3)} - 2\,W^n_{j,i(2:3)} + W^n_{j,i(1:3)}\right] \tag{8}$$

$$\lambda_4 = \frac{1}{4}E\left[W^n_{j,i(4:4)} - 3\,W^n_{j,i(3:4)} + 3\,W^n_{j,i(2:4)} - W^n_{j,i(1:4)}\right] \tag{9}$$

The notations $W^n_{j,i(q:r)}$ denotes the qth smallest value from a data set of r elements.

From the L-moment ratio diagram, the three-parameter generalized logistic distribution function was identified to fit the $W^n_{j,i}$ series at all the five timescales. The GLO is given in Eq. (10) (Hosking and Wallis 2005);

$$f\left(W^n_{j,i}\right) = \frac{\alpha^{-1}\exp\left[-(1-k)Y\right]}{\left[1+\exp\left(-Y\right)\right]^2} \tag{10}$$

$$Y = \begin{cases} -k^{-1}\log\left[1 - \frac{k\left(W^n_{j,i}-\xi\right)}{\alpha}\right], & k \neq 0 \\ \frac{\left(W^n_{j,i}-\xi\right)}{\alpha}, & k = 0 \end{cases} \tag{11}$$

The cumulative density distribution function from which probabilities of non-exceedance are derived is given by;

$$F\left(W^n_{j,i}\right) = \frac{1}{\left[1+\exp\left(-Y\right)\right]} \tag{12}$$

where k-shape, α-scale and ξ denotes location parameters which are obtained as functions of L-moments as follows;

$$k = -\tau_3 \tag{13}$$

$$\alpha = \frac{\lambda_2 \sin k\pi}{k\pi} \tag{14}$$

$$\xi = \lambda_1 - \alpha\left(\frac{1}{k} - \frac{\pi}{\sin k\pi}\right) \tag{15}$$

The probabilities of non-exceedance are then standardized through a Gaussian transformation into a normal variable through the following approximation by Abramowitz and Stegun (1964)

$$\mathrm{SPEI} = Z - \frac{2.516 + 0.803Z + 0.0103Z^2}{1 + 1.433Z + 0.189Z^2 + 0.0013Z^2} \tag{16}$$

where

$$Z = \left[\ln\left(\frac{1}{P^2}\right)\right]^{\frac{1}{2}} \tag{17}$$

where P is the probability of exceedance of a given $W^n_{j,i}$ value. The P value is obtained from $P = 1 - F(W^n_{j,i})$.

SPEI series are standardized with mean of zero and standard deviation of one for easier comparison on temporal and spatial scales. At each timescale, SPEI events which are continuously negative signify drought conditions defined for its duration, magnitude and intensity.

2.5 The influence of ENSO on drought severity

The influence of ENSO on drought severity represented by SPEI across the study area is investigated through the degree of association between the two variables at each of the respective timescale of 1, 3, 6, 12 and 24 month. The Pearson's correlations are obtained between SPEI and SSTs anomalies on one hand and SOI on the other hand at 95% confidence level. Correlations are performed with time series at a monthly scale to reveal any possible seasonality in the relationships. The results from this analysis have been presented in box and whisker plots.

3 Results

3.1 Drought temporal evolutions

SPEI time series are generated and used to characterize drought based on duration and magnitude. An event is classified as a drought when the SPEI values are persistently negative and terminates when the values become positive. With this, the onset and cessation of drought can be marked. Drought duration is taken as the time period during which the SPEI values are continuously negative while its magnitude is the total SPEI sum during the period of moisture deficit. The temporal characteristics have been determined at each of the 14 synoptic stations at timescales of 1, 3, 6, 12 and 24 month. For purposes of this paper, four representative stations evenly spread across the study area are presented here. These stations include: Francistown in the east, Ghanzi in the west, Shakawe in the north and Tsabong in the south. The drought temporal characteristics are presented in Figs. 2 and 3. In these plots, the evolutions at SPEI-1 are not presented due to their similarity with SPEI-3. Besides the SPEI-1 are only representing monthly variations that may not give a clear picture on drought effect when it persists within a given a given subsystem.

From Figs. 2 and 3, drought and humid periods were recorded regardless of the timescale. From these temporal evolutions, the historical droughts of 1962 to 1965 in the east that extended over the year in the south and in the western locations are well represented. The next drought event also reported on the plots is that of 1968 to 1970. This drought was recorded in all the regions though not well pronounced in the eastern region. The drought evolutions ably captured another historical drought of 1980 to 1985 that persisted for another 2 years in the west, north and southern locations. This drought event was interrupted in 1984–1985 with occasional humid periods. The eastern region recorded another dry spell between 1989 and 1995. This particular drought extended for another 2 years to 1997 in the west. In the north this drought event was delayed until 1993 but extended into 1999. The southern locations recorded this drought for 7 years from 1991 to 1997. The period between 2001 and 2007 was characterized by intermittent droughts in Botswana with most of these droughts lasting just under 12 month. The only period that recorded a longer duration was that dry spell of 2001 to 2004. Also from these plots, the most recent severe drought that ravaged Southern Africa of 2014–2016 is well represented. From these

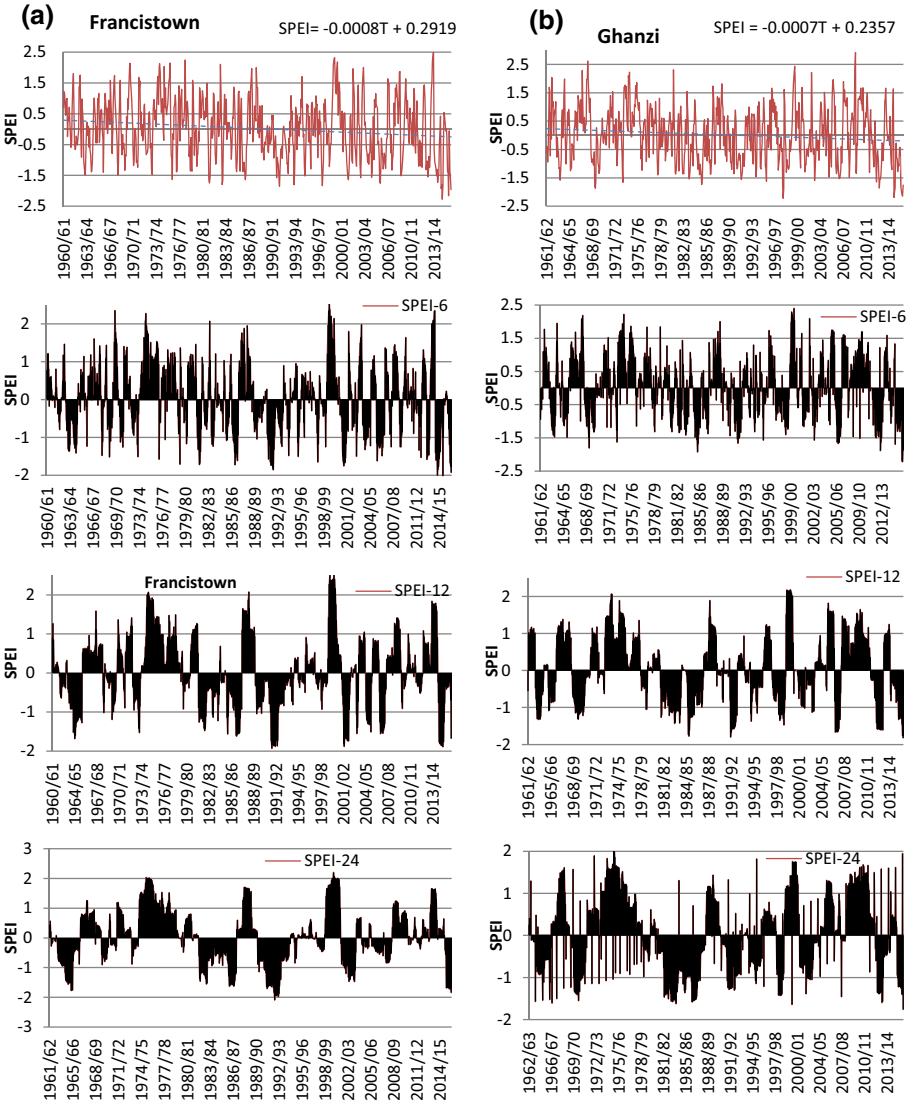

Fig. 2 Temporal evolution of SPEI of 3, 6, 12 and 24 month at **a** Francistown and **b** Ghanzi. Blue dotted line shows trends

evolutions, it is evident there is more severe and frequent droughts after 1980 to the present period.

The evolutions equally report humid conditions at the same time. From these plots it can be observed that the period between 1966 and 1968 was occasioned with wet spells across the study area. The longest wet spell on record was that between 1973 and 1978. This wet period even started earlier in 1971 for the eastern locations. This entire wet period was well captured by evolutions at all the locations shown in Figs. 2 and 3. Another wet spell that was recorded is between 1987 and 1989. This wet spell extended up to 2001 in the east

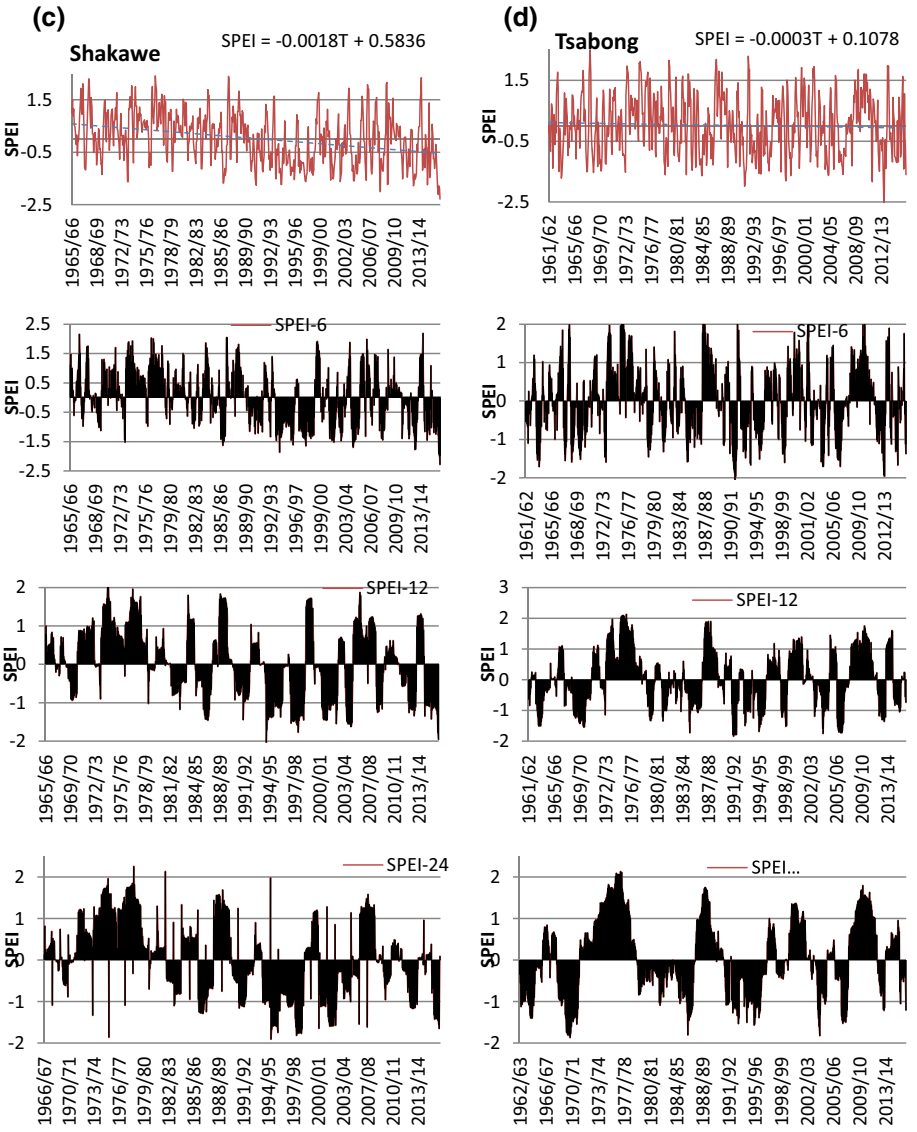

Fig. 3 Temporal evolution of SPEI of 3, 6, 12 and 24 month at **c** Shakawe and **d** Tsabong. Blue dotted line shows trends

with the western location recording the highest peak in 1999/2000 during the historical period. This event was well captured in other locations but not the most extreme. The most recent wet spell across Botswana was between 2009 and 2012 which was more pronounced in most regions apart from the east and the north that show intermittent humid periods.

Also included on the plots is a linear trend analysis for selected locations. These linear trends do indicate a negative gradient at all the locations for the period of analysis. A negative gradient depicts increasing drought severity towards the recent period. The east and

west show increasing drought trends at a drying rate of approximately 0.8% per decade. The southern region presents with a lower rate of 0.3% per decade of increasing drying trends. The northern locations show a higher increasing trend (1.8% per decade) than the rest of the locations but this may not be the case since the start period of trend analysis is later than for the rest of the locations.

3.2 Drought characteristics and vulnerability

As mentioned earlier, droughts have been categorized according to classifications in Table 1 as extreme, severe and moderate. Based on these classifications, drought occurrence probabilities have been determined. These probabilities are also an indication of a degree of drought vulnerability towards a specific drought category. In Table 2, the results of these drought probabilities are presented. These results show that severe and moderate categories of droughts are the most common in Botswana. Extreme droughts present with very little chance of occurrence with probabilities less than 1.0% recorded at most of the stations. It is only at Lethlakane that probabilities of 1.1% and 1.5% were realized at timescales of 1 and 3 month for the extreme drought category. Shakawe recorded the highest probability of 18.6% at 12 month timescale under the moderate drought category. High tendencies of vulnerability are also experienced at Mahalapye with probabilities of approximately 15.0% at 6 month timescale. The highest severe drought probability of 7.3% is recorded at 12 month timescale at Francistown. Equally Kasane shows higher tendencies towards this drought category of more than 5% at 3 and 12 month timescale.

Figures 4 and 5 present the spatial patterns of probabilities of various drought categories. Since it has been indicated earlier that only moderate and severe droughts are the most common in Botswana, only results for these two categories are presented here. For the 1 month timescale as shown in Fig. 4a, the north-western and eastern locations show a high degree of vulnerability towards severe droughts compared to other locations across the country. At the same timescale, moderate drought vulnerability presented in Fig. 4b indicate that the south-west, south and north-west show high tendencies of susceptibility towards this drought category.

For the 3 month timescale presented in Fig. 4c under the severe drought category it is mainly the north-eastern, eastern and southern locations that are more vulnerable. South-east towards the west show low vulnerability. Figure 4d for the moderate drought category contrasts the severe drought with the western locations starting north-west at Shakawe, Ghanzi in the west and Tsabong in the south-west all located in the Kalahari desert showing high vulnerability towards this drought category. Selibe-Phikwe and Mahalapye located in the south-east are equally vulnerable to this drought category. The spatial patterns also indicate that the eastern and southern locations of Jwaneng are not at threat from this drought category at 3-month timescale.

For the 6-month timescale, severe drought in contrast with the 3-month timescale, the eastern and southern locations are more vulnerable than the rest of other locations. However, the north-western and south-eastern locations that were seen vulnerable at the lower timescales are less susceptible. For the moderate drought category at 6-month timescale (Fig. 4f), the locations in the Kalahari desert still show high vulnerability towards this drought category. Locations in the north-east and central at Pandamatenga and Lethlakane, respectively, also show susceptibility towards this drought category. In the same vain, south-east at Selibe-Phikwe also show a high degree of vulnerability towards moderate droughts at this timescale.

Table 2 Probabilities of occurrence for extreme, severe and moderate droughts

Station	SPE1-1			SPE1-3			SPE1-6			SPE1-12			SPE1-24		
	Extm.	Sev.	Mod.	Extm.	Sev.	Mod.	Extm.	Sev.	Mod.	Extm.	Sev.	Mod.	Extm.	Sev.	Mod.
Francistown	0.6	4.5	10.3	0.3	4.5	11.5	0.3	5.2	11.7	0.0	7.3	7.9	0.2	7.2	6.3
Ghanzi	0.8	3.2	12.4	0.8	3.5	12.8	0.3	3.5	13.9	0.0	4.8	13.9	0.0	4.1	14.4
Jwaneng	0.6	3.1	12.3	0.3	4.7	9.6	0.0	5.0	11.6	0.0	3.8	13.7	0.0	7.0	9.3
Kasane	0.5	3.8	9.8	0.3	5.1	10.2	0.5	4.1	10.2	0.5	6.5	8.1	0.5	3.8	9.1
Letlhakane	1.1	3.4	11.0	1.5	3.4	12.2	0.4	3.5	14.3	0.4	4.3	11.5	0.0	4.6	10.8
Mahalapye	0.6	3.7	12.8	0.7	3.7	11.5	0.2	4.3	12.3	0.0	4.2	13.8	0.0	4.3	15.7
Maun	0.7	3.8	11.3	0.3	4.3	11.8	0.2	4.3	11.0	0.2	5.2	10.5	0.2	5.1	10.7
Pandamatenga	0.9	3.2	10.6	0.0	4.2	11.2	0.0	2.4	15.2	0.0	3.9	12.7	0.0	2.6	13.0
Selibe-Phikwe	0.5	2.6	12.0	0.0	2.1	12.6	0.0	2.1	13.4	0.0	5.0	12.2	0.0	6.5	9.5
Shakawe	0.5	4.2	11.8	0.5	4.6	12.6	0.2	2.5	16.0	0.2	2.8	18.6	0.0	5.9	12.9
SSKA	0.3	3.5	11.8	0.3	3.8	12.2	0.0	4.9	12.3	0.0	4.4	14.7	0.0	5.4	12.0
Sowa Pan	0.0	3.8	11.8	0.7	3.8	10.8	0.0	6.0	9.9	0.0	3.2	14.8	0.0	4.9	10.2
Tsabong	0.6	2.7	12.3	0.3	3.8	12.9	0.2	4.4	13.8	0.0	4.5	14.3	0.0	3.0	14.6
Tshane	0.6	2.9	13.2	0.2	4.7	12.3	0.0	4.4	11.9	0.0	6.8	9.7	1.4	3.6	9.1

Extm. extreme drought, *Sev.* severe drought, *Mod.* moderate drought

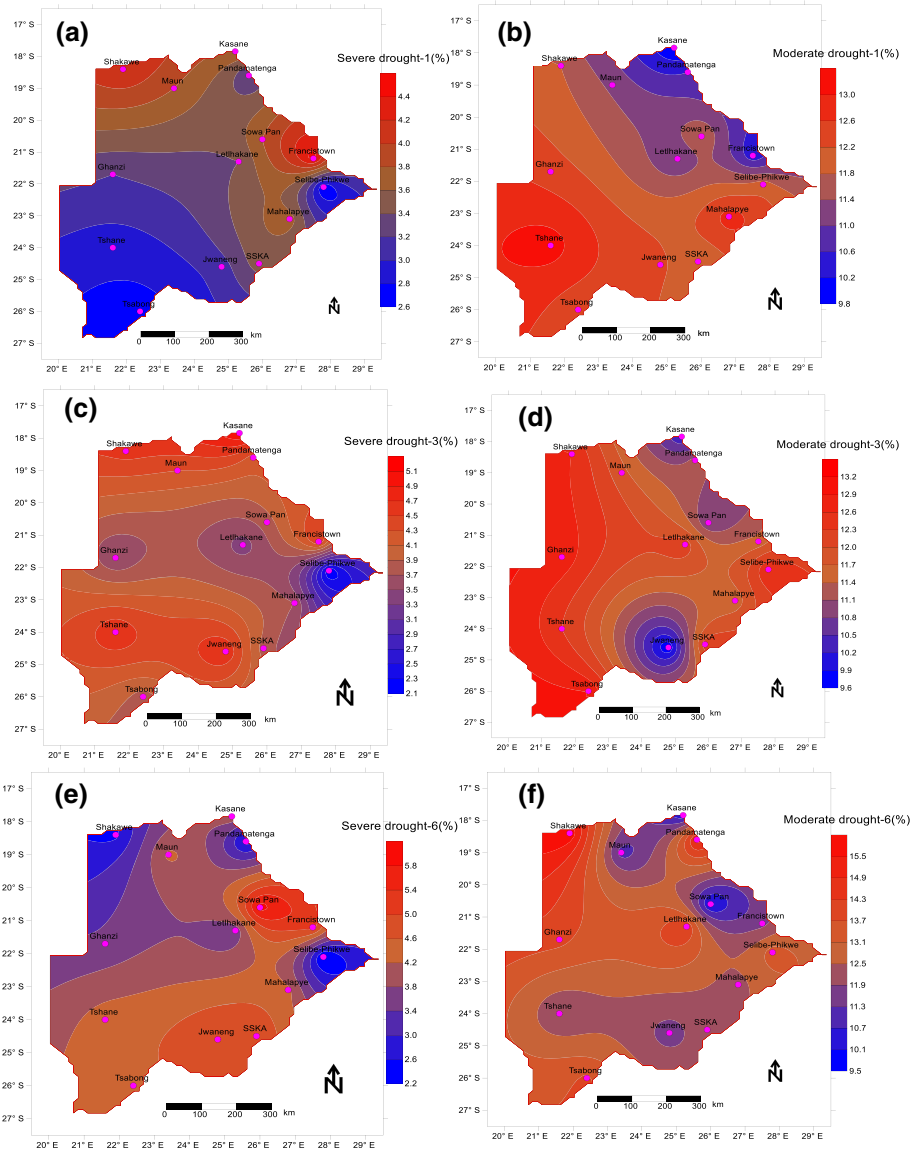

Fig. 4 Spatial representation of vulnerability towards **a** SPEI-1 severe drought, **b** SPEI-1 moderate drought, **c** SPEI-3 severe drought **d** SPEI-3 moderate drought, **e** SPEI-6 severe drought **f** SPEI-6 moderate drought

For the 12-month timescale, Fig. 5a presents the spatial distribution of severe drought probabilities indicating that a large part of the study area is not vulnerable to this drought category. Selected locations like Kasane, Tshane and Francistown show elements of susceptibility. Moderate droughts at the same timescale in Fig. 5b show a larger spatial extent of vulnerability towards this drought category compared severe droughts.

For the 24-month timescale in Fig. 5c (for severe droughts) the north-west to south-east shows higher tendencies of drought vulnerability towards this drought category. For the

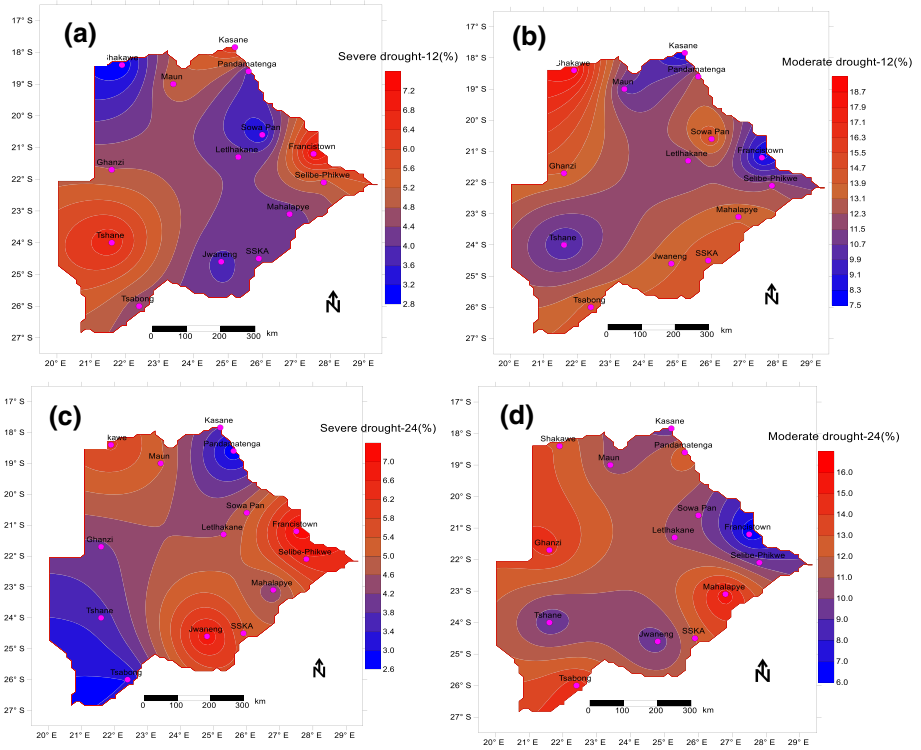

Fig. 5 Spatial representation of vulnerability towards **a** SPEI-12 severe drought, **b** SPEI-12 moderate drought, **c** SPEI-24 severe drought **d** SPEI-24 moderate drought

moderate droughts presented in Fig. 5d, the north-west and south-east are the most susceptible areas towards this drought category.

3.3 Association of ENSO and drought severity

The ENSO influence represented by SST anomalies and SOI on the local climate has been investigated with Pearson's correlations. Results from this analysis are presented in box and whisker plots in Figs. 6 and 7. Figure 6 shows correlation between SPEI and SST anomalies at timescales of 1, 3, 6, 12 and 24 month. This relationship mostly returned negative correlations between SPEI and SST. In January, statistically significant correlations were strongest. Correlations during this month range from −0.8 to −0.3 at 1 and 24 month timescale, respectively. These correlations lower (−0.6 to −0.3) in the subsequent months of February and March. At the end of the rain season in April, correlations cease to be statistically significant moving through winter months of May, June, July and August. During this period, correlations are weak and at times positive indicating a nonexistent relationship between SSTs and SPEI. Drought in Southern Africa is mainly attributed to a combination of negative SPEI and positive SST anomalies (Vicente-Serrano et al. 2011). October which marks the onset of rains in Botswana, non-significant negative correlations start to emerge becoming significant in December. The peak correlations in December range from −0.7 to −0.5 at 1 and 24 months, respectively.

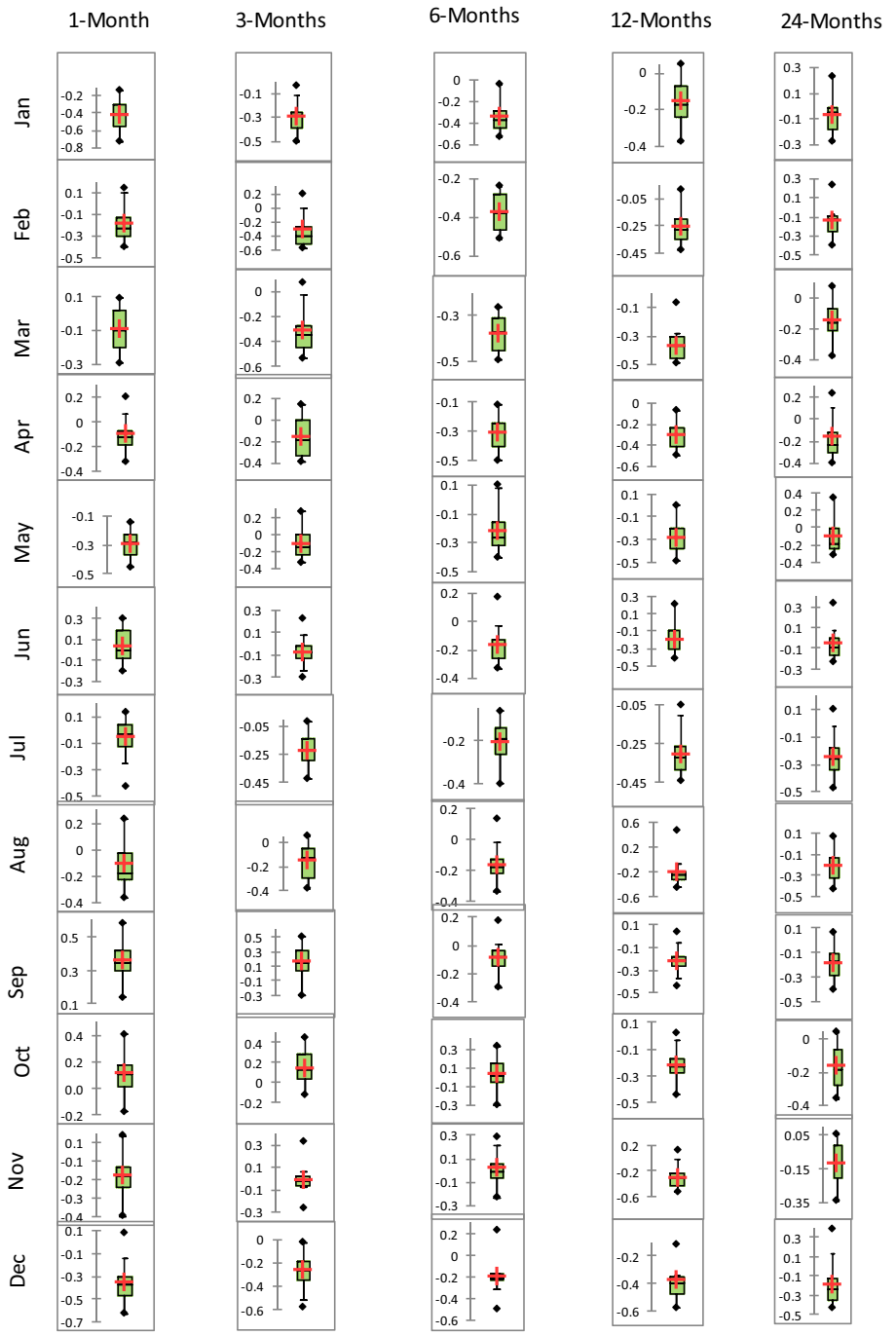

Fig. 6 Box and whisker plots of the Pearson's correlation coefficients between SPEI and SSTs

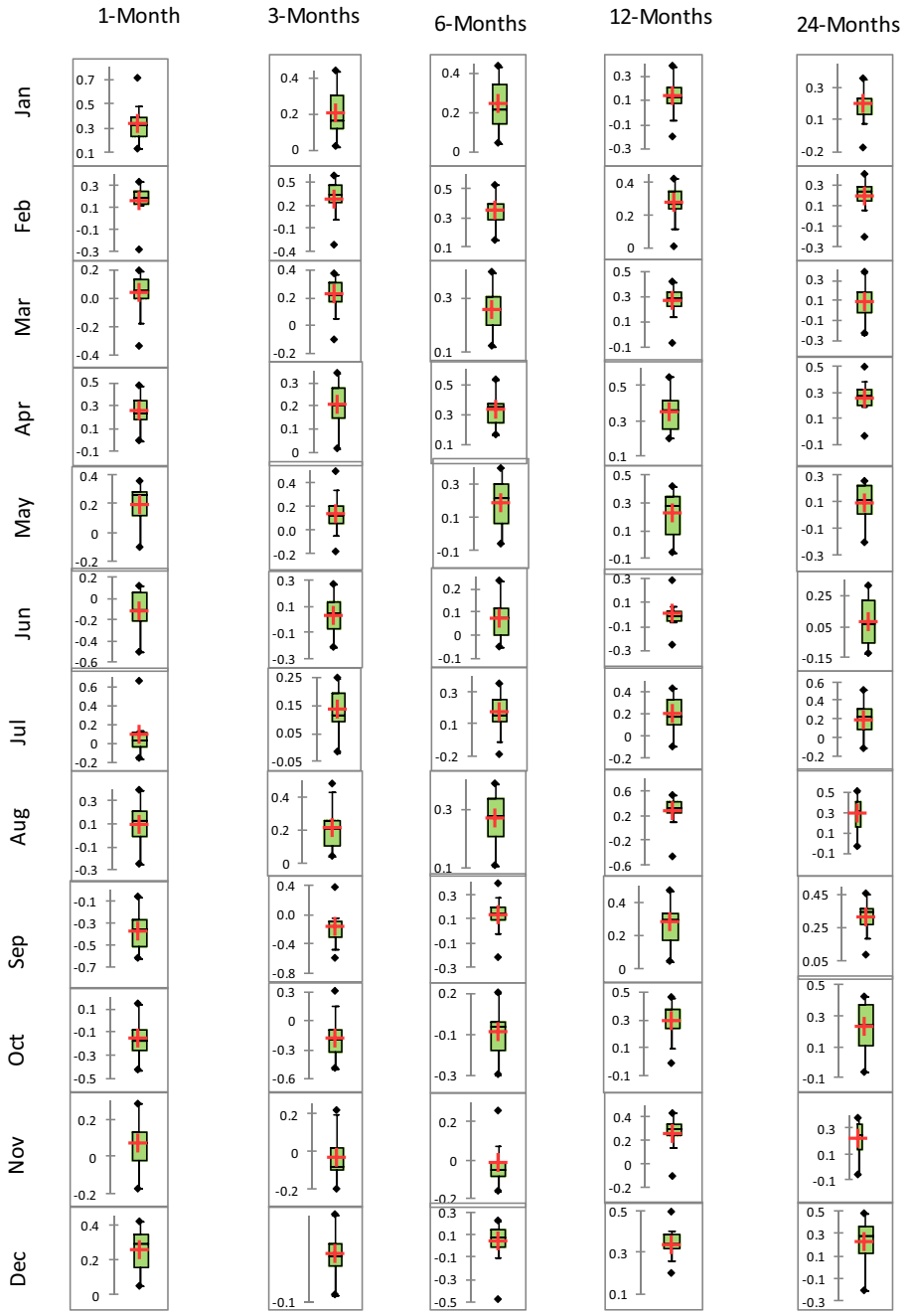

Fig. 7 Box and whisker plots of the Pearson's correlation coefficients between SPEI and SOI

Results of the relationship between SPEI and SOI on the other hand are presented in Fig. 7. These results show mainly positive correlations between the climatic variables. Positively significant correlations were mainly recorded during summer months. The significant and highest correlations were recorded in January ranging from 0.7 to 0.3 at 1 and 24 month, respectively. During the subsequent months of February and March, correlations range from 0.6 to 0.2 following similar trends as those between SPEI and SST. During winter, non-significant correlations are recorded and in some instances negative values resulted. Correlations start to increase in November becoming significant in December ranging between 0.5 and 0.3 across timescales.

SST anomaly and SOI are also plotted together with SPEI-12 at Tsabong synoptic station in Fig. 8 so as to illustrate temporal evolution patterns. These results demonstrate that a warm SST combined with negative SOI corresponds to persistent negative SPEI values and hence drought. From the graphs, droughts attributed to El Niño years on record in Southern Africa of 1963/64, 1965/66, 1968/69, 1969/70, 1979/80, 1982/83, 1986/87, 1991/92,

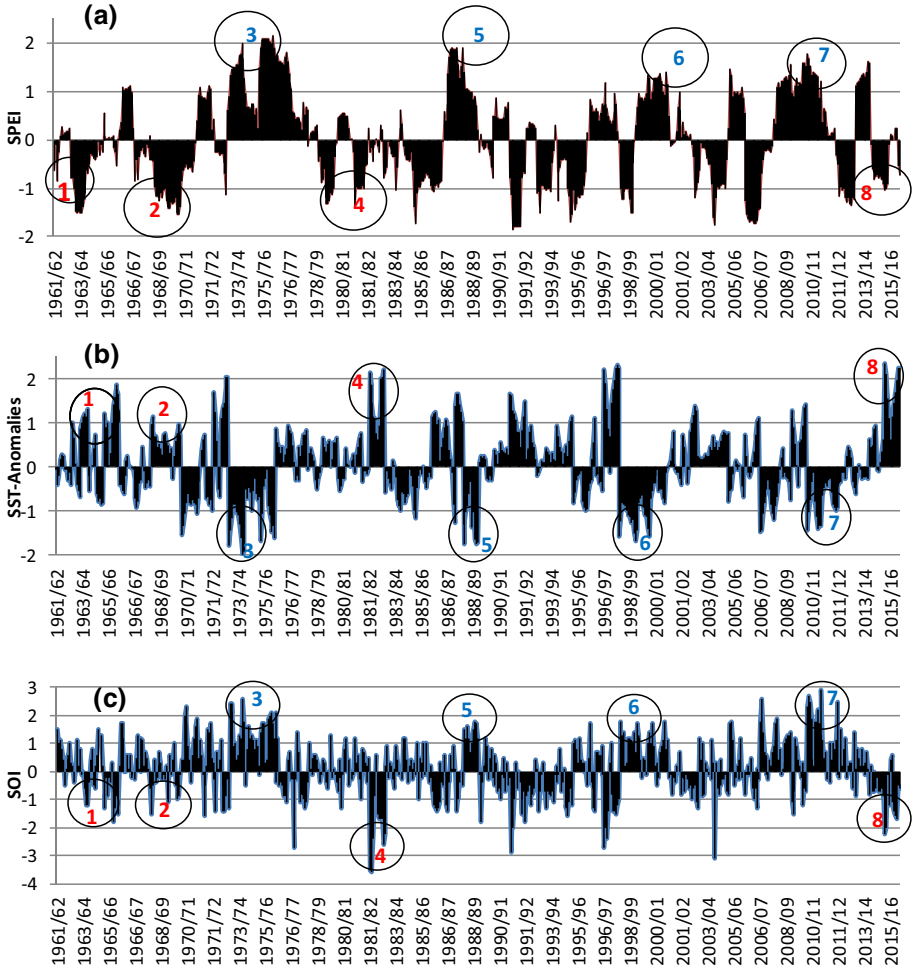

Fig. 8 Temporal evolutions comparing SPEI and ENSO **a** SPEI-12 at Tsabong **b** SST anomalies and **c** SOI

1997/88, 1988/89, 2004/05, 2006/07, 2014/15 and 2015/16 are well pronounced. Wet and dry events have been marked 1–8 in Fig. 8. Events marked 1 corresponds to El Niño years of 1963/64 and 1965/66, events marked 2 coincided with El Niño years of 1968/69 and 1969/70 while events marked 4 corresponds to El Niño years of 1979/80 and 1982/83. Also event marked 8 corresponds to the recent El Niño years of 2014/15 and 2015/16. Strong positive SST anomalies corresponding to strong negative SOI which also are observed to align with severe drought conditions (negative SPEIs). This is a clear manifestation that drought episodes closely follow El Niño events. Events marked 1, 2, 4 and 8 in Fig. 8a corresponds to dry spells at Tsabong, compared to the same period marked red in Fig. 8c, the periods are marked with negative SOIs and Fig. 8b is marked with warm anomalies for the same period. Events marked 3, 5, 6 and 7 in Fig. 8a corresponds to wet periods (positive SPEIs) aligns with positive SOI and negative SSTs in Fig. 8c and b, respectively, depicting wet spells.

4 Discussions

4.1 Drought temporal evolutions

Results have indicated that temporal evolutions of droughts take different forms across timescales at the same location. Drought evolutions at lower timescales of 1 and 3 month exhibited higher frequency compared to those at higher timescales of 6, 12, and 24 month. This result agrees with those from similar studies such as those of Yu et al. (2014), Vicente-Serrano et al. (2015) and most recently by Byakatonda et al. (2018b). These studies were conducted in China, Bolivia and Botswana, respectively. Both humid and drought periods are reported to occur in Botswana during the historical period. These events occurred uniformly across the study area. This uniformity could be attributed to Botswana's flat topography that facilitates uniform atmospheric circulation. Also studying drought characteristic at various timescales aids understanding of the creeping nature of droughts and its propagation mechanism. Drought propagates from meteorological to agricultural droughts at lower timescales of 1 and 3 month. At higher timescales of 12 and 24 month, drought effects on the hydrological and environmental systems can be felt (Nalbantis and Tsakiris 2009; Lorenzo-Lacruz et al. 2010; Van Loon 2013; Trambauer et al. 2014). This then demonstrates that temporal evolutions could be useful in drought monitoring. In turn, this mitigates their impacts on various components of the hydrological cycle.

The foregoing results also indicate that there have been more frequent droughts after 1980/81 compared to the previous period. This could be in relation to the findings of Parida and Moalafhi (2008) and Byakatonda et al. (2018b) who reported an intervention in rainfall, minimum and maximum temperature time series across Botswana during the same time period. Humid and dry spells on the plots sometimes coincided with El Niño for dry periods or La Niña for humid spells. To mention a few, the La Niña years of 1976/68, 1973/74, 1999/00 and 2010/11 corresponded with humid periods shown on the plots. Similarly, some of the El Niño years occurred during drought years such as 1963/64, 1982/83, 1994/95, 2002/03, 2004/05, 2006/07 and the most recent of 2015/16. Some of these historical droughts have also been widely reported on the African continent in Masih et al. (2014). The most recent drought/El Niño has also been identified by Hansen et al. (2016) as the year with the strongest El Niño in 100 years. This could be evidence that

large climatic predictors have a direct influence on drought characteristics of mainland Botswana. Besides, Nicholson et al. (2001) and Usman and Reason (2004) had already reported a possible influence of ENSO on South Africa's climate. Since these findings corroborate each other, Botswana is highly likely to be affected directly by climatic variability as a result of ENSO activities in the equatorial Pacific.

4.2 Drought characteristics and vulnerability

According to the results, Botswana is vulnerable to two drought categories viz: severe and moderate droughts. Earlier studies of drought assessment using SPI by Batisani (2011) had reported that Botswana was indeed more vulnerable to moderate droughts. The fact the SPI only uses rainfall in quantification of droughts it could imply that droughts in Botswana are attributed to low or lack of rainfall than the ongoing phenomena of global warming. The north including Pandamatenga and Sowa Pan are identified to be highly vulnerable to drought. These locations have also been identified by Byakatonda et al. (2019) as potential areas for rainfed agriculture. This revelation could hamper efforts towards improving the food security situation in Botswana. The results also reveal that vulnerability increased up to 12 month timescale which could also mean that the over the year timescales may not be necessary in drought monitoring across the study area. The western locations on the fringes of the Kalahari desert such as Shakawe, Ghanzi and Tsabong are presenting with the highest degree of vulnerability compared to other locations. But also it is further reported that locations of Ghanzi and Tsabong receive the lowest amounts of rainfall in Botswana. Investigations by Pachauri and Reisinger (2007) and Stocker et al. (2013) indicate that with the current global warming, there is a likely shift in atmospheric circulation with dry locations getting even drier. This creates more uncertainties in these locations which may degenerate into hyper arid climates and hence threatening livelihood. Given the susceptibility of region to climate extremes, institutions such as the South African Development Community Drought Monitoring Centre (SADC-DMC), under the guidance from WMO, was established in order to contribute to the mitigation of the negative impacts of drought or floods over the region. The SADC-DMC generates and disseminates important outputs such as 10 day forecast bulletins and seasonal rainfall outlooks, as a contribution to mitigation of negative impacts of extreme climatic anomalies. SADC-DMC has the responsibility of monitoring and prediction of the global and regional climate system. The current research augments efforts of the SADC-DMC and therefore helps the government of Botswana to better monitor droughts.

4.3 Association of ENSO with drought severity

A negative relationship between SPEI and SSTs demonstrates that negative anomalies of SSTs associated with El Niño correspond with negative SPEI attributed to drought conditions. Equally positive SPEI responsible for humid conditions corresponds with positive SOI which is responsible for La Niña conditions. These relationships corroborate findings from studies over Southern Africa conducted by Nicholson et al. (2001), Trenberth et al. (2007), Vicente-Serrano et al. (2011) and Byakatonda et al. (2018b) that reported influence of ENSO on regional climate. Significant correlations were mainly during summer which also coincides with the rain season in Botswana. This could mean that the rainfall totals received during a particular summer could be directly related to the Ocean Niño Index (ONI) of region 3.4 of the equatorial Pacific. In contrast, correlations during the winter

season showed no relationship between SPEI and ENSO, which implies that climate variability during this season may not be explained by ENSO but rather with other global circulation mechanisms.

5 Conclusions

This study has characterized droughts in Botswana together with their spatial distribution using SPEI. Probabilities of occurrence have been used to assess the degree of drought vulnerability with its spatial extent also presented to facilitate drought monitoring and planning. The study has shown a close relationship between Botswana's summer climate and ENSO. From the foregoing results and discussions, the following summary has been deduced.

1. The variations between drought and humid events were distinct across the timescales of 1, 3, 6, 12, and 24 month that were used in the analysis. Lower timescales of 1 and 3 month have higher temporal variations compared to 12 and 24 month. It was also observed that drought events increased in both frequency and severity after 1980/81 in most cases coinciding with El Niño years.
2. The northern locations and the fringes of the Kalahari desert were more susceptible to moderate droughts in Botswana. Vulnerabilities increased with timescale up to 12 month.
3. Botswana's climate is mainly associated with ENSO during the summer months with the highest association occurring in December and January the peak of the rain season.

From the summary above, this study is critical to drought preparedness and planning. Because of the significant relationship between drought severity and ENSO, the drought early warning systems could use ENSO for predicting drought and hence used in drought management in Botswana.

Acknowledgements The authors wish to thank the Mobility for Engineering Graduates in Africa (METEGA) for funding this study. We also pass our gratitude to the editor and anonymous reviewers for their insights in an effort to improve the quality of the manuscript. The Department of Meteorological services (DMS) of Botswana provided the climatological data used in this study for this we are grateful.

References

Abramowitz M, Stegun IA (1964) Handbook of mathematical functions: with formulas, graphs, and mathematical tables. Courier Corporation, North Chelmsford

Alexandersson H (1986) A homogeneity test applied to precipitation data. J Climatol 6:661–675

Allen RG, Pereira LS, Raes D, Smith M (1998) FAO Irrigation and drainage paper no. 56. Rome Food Agric Organ UN 56:97–156

Alley WM (1984) The Palmer drought severity index: limitations and assumptions. J Clim Appl Meteorol 23:1100–1109

Batisani N (2011) The spatio-temporal-severity dynamics of drought in Botswana. J Environ Prot (Irvine, Calif) 2:803

Batisani N (2012) Climate variability, yield instability and global recession: the multi-stressor to food security in Botswana. Clim Dev 4:129–140

Beguería S, Vicente-Serrano SM, Reig F, Latorre B (2014) Standardized precipitation evapotranspiration index (SPEI) revisited: parameter fitting, evapotranspiration models, tools, datasets and drought monitoring. Int J Climatol 34:3001–3023. https://doi.org/10.1002/joc.3887

Bepura C (1999) Drought management: a SADC perspective. In: Proceedings of the international conference on integrated drought management: lessons for sub Saharan Africa, 20–22 Sept

Bromwich DH, Rogers AN, Kallberg P et al (2000) ECMWF analyses and reanalyses depiction of ENSO signal in Antarctic precipitation. J Clim 13:1406–1420. https://doi.org/10.1175/1520-0442(2000)013%3c1406:EAARDO%3e2.0.CO;2

Byakatonda J, Parida BP, Kenabatho PK, Moalafhi DB (2016) Modeling dryness severity using artificial neural network at the Okavango Delta, Botswana. Glob Nest J 18:463–481

Byakatonda J, Parida BP, Kenabatho PK, Moalafhi DB (2018a) Analysis of rainfall and temperature time series to detect long-term climatic trends and variability over semi-arid Botswana. J Earth Syst Sci 127:25. https://doi.org/10.1007/s12040-018-0926-3

Byakatonda J, Parida BP, Moalafhi DB, Kenabatho PK (2018b) Analysis of long term drought severity characteristics and trends across semiarid Botswana using two drought indices. Atmos Res. https://doi.org/10.1016/j.atmosres.2018.07.002

Byakatonda J, Parida BP, Kenabatho PK, Moalafhi DB (2019) Prediction of onset and cessation of austral summer rainfall and dry spell frequency analysis in semiarid Botswana. Theor Appl Climatol 135:101–117

Cai J, Liu Y, Lei T, Pereira LS (2007) Estimating reference evapotranspiration with the FAO Penman–Monteith equation using daily weather forecast messages. Agric For Meteorol 145:22–35

Conforti P, Ahmed S, Markova G et al. (2018) Impact of disasters and crises on agriculture and food security- 2017. FAO, Rome, Italy

Costa AC, Soares A (2009) Homogenization of climate data: review and new perspectives using geostatistics. Math Geosci 41:291–305. https://doi.org/10.1007/s11004-008-9203-3

Dai A (2013) Increasing drought under global warming in observations and models. Nat Clim Change 3:52–58

Edossa DC, Woyessa YE, Welderufael WA (2014) Analysis of droughts in the central region of South Africa and their association with SST anomalies. Int J Atmos Sci 2014:508953

Engelbrecht F, Adegoke J, Bopape M-J et al (2015) Projections of rapidly rising surface temperatures over Africa under low mitigation. Environ Res Lett 10:85004

FAO (2001) Drought impact mitigation and prevention in the Limpopo River Basin: a situation analysis. FAO, Rome

Fauchereau N, Trzaska S, Rouault M, Richard Y (2003) Rainfall variability and changes in southern Africa during the 20th century in the global warming context. Nat Hazards 29:139–154

Feidas H, Makrogiannis T, Bora-Senta E (2004) Trend analysis of air temperature time series in Greece and their relationship with circulation using surface and satellite data: 1955–2001. Theor Appl Climatol 79:185–208

Franks SW (2005) Regional hydrological impacts of climatic change: impact assessment and decision making. International Association of Hydrological Sciences, Foz do Iguaço, Brazil

Guha-Sapir D, Below R, Hoyois P (2016) EM-DAT: the CRED/OFDA international disaster database. In: UN Environ. Doc. Repos.

Hansen J, Sato M, Ruedy R et al (2016) Global temperature in 2015. GISS, NASA, New York, pp 1–6

Hayes M, Svoboda M, Wall N, Widhalm M (2011) The Lincoln declaration on drought indices: universal meteorological drought index recommended. Bull Am Meteorol Soc 92:485–488

Heim RR Jr (2002) A review of twentieth-century drought indices used in the United States. Bull Am Meteorol Soc 83:1149–1165

Hosking JRM, Wallis JR (2005) Regional frequency analysis: an approach based on L-moments. Cambridge University Press, Cambridge

Iglesias A, Garrote L, Cancelliere A et al (2009) Coping with drought risk in agriculture and water supply systems: drought management and policy development in the Mediterranean. Springer, Berlin

Lloyd-Hughes B (2012) A spatio-temporal structure-based approach to drought characterisation. Int J Climatol 32:406–418

Lorenzo-Lacruz J, Vicente-Serrano SM, López-Moreno JI et al (2010) The impact of droughts and water management on various hydrological systems in the headwaters of the Tagus River (central Spain). J Hydrol 386:13–26

Masih I, Maskey S, Mussá FEF, Trambauer P (2014) A review of droughts on the African continent: a geospatial and long-term perspective. Hydrol Earth Syst Sci 18:3635

Mbululo Y, Nyihirani F (2012) Climate characteristics over southern highlands Tanzania. Atmos Clim Sci 2:454–463. https://doi.org/10.4236/acs.2012.24039

McEvoy DJ, Huntington JL, Abatzoglou JT, Edwards LM (2012) An evaluation of multiscalar drought indices in Nevada and Eastern California. Earth Interact 16:1–18
McKee TB, Doesken NJ, Kleist J, et al (1993) The relationship of drought frequency and duration to time scales. In: Proceedings of the 8th conference on applied climatology, pp 179–183
Mishra AK, Singh VP (2010) A review of drought concepts. J Hydrol 391:202–216
Morchain D, Urquhart P, Zaremba J (2017) Background paper on Botswana's draft drought management strategy. Gaborone, Botswana
Morid S, Smakhtin V, Bagherzadeh K (2007) Drought forecasting using artificial neural networks and time series of drought indices. Int J Climatol 27:2103–2111
Nalbantis I, Tsakiris G (2009) Assessment of hydrological drought revisited. Water Resour Manag 23:881–897
Narasimhan B, Srinivasan R (2005) Development and evaluation of Soil Moisture Deficit Index (SMDI) and Evapotranspiration Deficit Index (ETDI) for agricultural drought monitoring. Agric For Meteorol 133:69–88
Nicholson SE, Kim J (1997) The Relationship of the El Niño Southern Oscillation To African Rainfall. Int J Climatol 17:117–135. https://doi.org/10.1002/(SICI)1097-0088(199702)17:2%3c117:AID-JOC84%3e3.0.CO;2-O
Nicholson SE, Leposo D, Grist J (2001) The relationship between El Niño and drought over Botswana. J Clim 14:323–335
NOAA-NCDC (2016) Southern Oscillation Index (SOI). www.ncdc.noaa.gov/teleconnections/enso/indicators/soi/data.csv. Accessed 16 Oct 2016
NOAA-NCEP (2016) Average sea surface temperetaure (SST) anormalies in region 3.4 of the Equatorial Pacific. http://www.cpc.ncep.noaa.gov/products/analysis_monitoring/ensostuff/ONI_change.shtml. Accessed 16 Oct 2016
Nyenzi B, Lefale PF (2006) El Nino southern oscillation (ENSO) and global warming. Adv Geosci 6:95–101
Pachauri RK, Reisinger A (2007) IPCC fourth assessment report. IPCC, Geneva
Parida BP, Moalafhi DB (2008) Regional rainfall frequency analysis for Botswana using L-Moments and radial basis function network. Phys Chem Earth 33:614–620. https://doi.org/10.1016/j.pce.2008.06.011
Pettit AN (1979) Anon-parametric approach to the change-point detection. Appl Stat 28:126–135
Potop V, Türkott L, Kožnarová V, Možný M (2010) Drought episodes in the Czech Republic and their potential effects in agriculture. Theor Appl Climatol 99:373–388
Rahman MR, Lateh H (2017) Climate change in Bangladesh: a spatio-temporal analysis and simulation of recent temperature and rainfall data using GIS and time series analysis model. Theor Appl Climatol 128:27–41. https://doi.org/10.1007/s00704-015-1688-3
Rojas O, Li Y, Cumani R (2014) An assessment using FAO's Agricultural Stress Index (ASI) understanding the drought impact of El Niño on the global agricultural areas. FAO, Rome, Italy
Sheffield J, Wood EF, Roderick ML (2012) Little change in global drought over the past 60 years. Nature 491:435–438
Sivakumar MVK, Motha R, Wilhite D, Wood D (2011) Agricultural drought indices. In: Proceedings of an expert meeting: 2–4 June, 2010, Murcia, Spain. WMO
Stagge JH, Tallaksen LM, Xu CY, Van Lanen HAJ (2014) Standardized precipitation-evapotranspiration index (SPEI): sensitivity to potential evapotranspiration model and parameters. In: Proceedings of the FRIEND-Water, pp 367–373
Stagge JH, Tallaksen LM, Gudmundsson L et al (2015) Candidate distributions for climatological drought indices (SPI and SPEI). Int J Climatol 35:4027–4040
Stocker TF, Qin D, Plattner GK, et al (2013) Climate change 2013: the physical science basis. Intergovernmental panel on climate change, working group I contribution to the IPCC fifth assessment report (AR5)
Trambauer P, Maskey S, Werner M et al (2014) Identification and simulation of space–time variability of past hydrological drought events in the Limpopo River basin, southern Africa. Hydrol Earth Syst Sci 18:2925–2942
Trenberth KE, Jones PD, Ambenje P et al (2007) Observations: surface and atmospheric climate change, chapter 3. IPCC, London, UK
Troup AJ (1965) The "southern oscillation". Q J R Meteorol Soc 91:490–506
Usman MT, Reason CJC (2004) Dry spell frequencies and their variability over southern Africa. Clim Res 26:199–211. https://doi.org/10.3354/cr026199
Van Loon AF (2013) On the propagation of drought: how climate and catchment characteristics influence hydrological drought development and recovery. Wageningen University, Wageningen

Vicente-Serrano SM, Begueria S, López-Moreno JI (2010) A multiscalar drought index sensitive to global warming: the standardized precipitation evapotranspiration index. J Clim 23:1696–1718
Vicente-Serrano SM, López-Moreno JI, Gimeno L et al (2011) A multiscalar global evaluation of the impact of ENSO on droughts. J Geophys Res. https://doi.org/10.1029/2011JD016039
Vicente-Serrano SM, Chura O, López-Moreno JI et al (2015) Spatio-temporal variability of droughts in Bolivia: 1955–2012. Int J Climatol. https://doi.org/10.1002/joc.4190
Wang W, Zhu Y, Xu R, Liu J (2015) Drought severity change in China during 1961–2012 indicated by SPI and SPEI. Nat Hazards 75:2437–2451
White DH, Walcott JJ (2009) The role of seasonal indices in monitoring and assessing agricultural and other droughts: a review. Crop Pasture Sci 60:599–616
Wijngaard JB, Klein Tank AMG, Können GP (2003) Homogeneity of 20th century European daily temperature and precipitation series. Int J Climatol 23:679–692
Wilhite DA, Svoboda MD, Hayes MJ (2007) Understanding the complex impacts of drought: a key to enhancing drought mitigation and preparedness. Water Resour Manag 21:763–774
WMO (2009) Guidelines on analysis of extremes in a changing climate in support of informed decisions for adaptation. WMO, Geneva
Yaghoobi AHZ (2012) Handling uncertainty in hydrologic analysis and drought risk assessment using Dempster–Shafer theory. University of British Columbia
Yu M, Li Q, Hayes MJ et al (2014) Are droughts becoming more frequent or severe in China based on the standardized precipitation evapotranspiration index: 1951–2010? Int J Climatol 34:545–558
Yuan J, Hartmann DL (2008) Spatial and temporal dependence of clouds and their radiative impacts on the large-scale vertical velocity profile. J Geophys Res. https://doi.org/10.1029/2007JD009722